Novel, cost-effective configurations of combined power plants for small-scale cogeneration from biomass: Feasibility study and performance optimization

NOVEL, COST-EFFECTIVE CONFIGURATIONS OF COMBINED POWER PLANTS FOR SMALL-SCALE COGENERATION FROM BIOMASS: FEASIBILITY STUDY AND PERFORMANCE OPTIMIZATION

Riccardo Amirante[1], Paolo Tamburrano[2]

[1,2] *Department of Mechanics, Mathematics and Management (DMMM)*

Polytechnic University of Bari, Italy

[1]*riccardo.amirante@poliba.it, +39 0805963470*

Abstract

The aim of this paper is to demonstrate that, thanks to recent advances in designing micro steam expanders and gas to gas heat exchangers, the use of small combined cycles for simultaneous generation of heat and power from the external combustion of solid biomass and low quality biofuels is feasible. In particular, a novel typology of combined cycle that has the potential both to be cost-effective and to achieve a high level of efficiency is presented. In the small combined cycle proposed, a commercially available micro-steam turbine is utilized as the steam expander of the bottoming cycle, while the conventional microturbine of the topping cycle is replaced by a cheaper automotive turbocharger. The feasibility, reliability and availability of the required mechanical and thermal components are thoroughly investigated. In order to explore the potential of such a novel typology of power plant, an optimization procedure, based on a genetic algorithm combined with a computing code, is utilized to analyze the trade-off between the maximization of the electrical efficiency and the maximization of the thermal efficiency. Two design optimizations are performed: the first one makes use of the innovative "Immersed Particle Heat Exchanger", whilst a nickel alloy heat exchanger is used in the other one. After selecting the optimum combination of the design parameters, the operation in load following mode is also assessed for both configurations.

Keywords

Combined heat and power, biomass, combined cycle, gas to gas heat exchanger, cogeneration

Nomenclature

c_p	*Specific heat at constant pressure*	*[J/(kg K)]*
G_a	*Air mass flow rate*	*[kg/s]*
G_s	*Steam mass flow rate*	*[kg/s]*
G_b	*Fuel mass flow rate*	*[kg/s]*
h	*Specific Enthalpy*	*[J/kg]*
h_b	*Initial specific enthalpy of the fuel*	*[J/kg]*
p	*Pressure*	*[bar]*
P_{el}	*Total electrical power*	*[kW]*
P_{th}	*Total useful thermal power*	*[kW]*
T	*Temperature*	*[K]*
ΔT_{pp}	*ΔT at pinch point*	*[K]*

β	*Air compression ratio*
ε	*Heat exchanger efficiency*
η_b	*Combustor efficiency*
η_{el}	*Overall electrical efficiency*
η_{is}	*Isentropic efficiency*
η_m	*Mechanical efficiency*
η_{th}	*Thermal efficiency*
η_{tot}	*Total efficiency*
x_s	*Dryness fraction of steam*
Acronyms	
CHP	*Combined heat and power*
HRSG	*Heat recovery steam generator*
IPHE	*Immersed particle heat exchanger*
LHV	*Lower heating value*
MOGAII	*Multi objective genetic algorithm II*
NAHE	*Nickel alloy heat exchanger*
ORC	*Organic Rankine Cycle*
PES	*Primary Energy Saving*
RPM	*Revolutions per minute*
Subscripts	
1	*Compressor inlet*
2	*Compressor outlet*
3	*Gas turbine inlet*
4	*Gas turbine outlet*
5	*Combustor exit*
6	*HRSG inlet (flue gas)*
7	*Exhaust*
bot	*Bottoming cycle*
c	*Compressor*
E	*Steam expander inlet*
e	*Expander*
K	*Water inlet in the HRSG*
F	*Steam expander outlet*
pp	*Pinch point in the HRSG*
sw	*Saturated water in the HRSG*
t	*Turbine*
top	*Topping cycle*

1. Introduction

Among renewable energy resources, biomass is largely available worldwide and is considered the one with the highest potential impact on the energy development [1]. A wider exploitation of biomass along with ever-increasing improvements in the capture and storage of carbon emitted by fossil fuels combustion plants (see, e.g, the membrane reactor analysed in [2]) can play a key role in preventing global warming. Biomass can be used either directly as solid fuel feeding power plants or indirectly after conversion into a secondary form of energy (e.g. syngas and biogas) by using air, oxygen and/or steam [3]. Because of its lower heating value and difficulties related to collection systems, packaging, transport and storage systems, biomass is best suited to small-scale power plants, where the electricity generation is coupled with the production of useful heat in order to compensate for the low electrical efficiency (typical of small power plants fed by biomass), thus increasing the total efficiency [4].

In addition to increasing eco-efficiency, such Combined Heat and Power (CHP) units for decentralized power generation eliminate the inefficiency of power transmission and distribution typical of centralized energy systems. Small-scale CHP systems with electrical power less than 100 kW_e are also particularly suitable for commercial buildings, hospitals, industrial premises, schools, office building, dwelling houses [5]. The demand for biomass in a small CHP plant can easily be satisfied by materials from surrounding areas, e.g. by exploiting agricultural and forestry residues, by-products of the food industry, residues from wood processing. Examples of how forest and agricultural biomass can be exploited profitably for small-scale energy production are provided in [6].

Despite all the potential benefits, the employment of CHP plants fed by biomass has not been so widespread as expected in those countries having large availability of biomass: apart from the above-mentioned difficulties in transport and storage systems along with uncertainties in feedstock availability and prices, this can be attributed to the high capital costs and long payback periods as well as the low ratio of electrical power to thermal power of typical CHP plants [7]. For instance, the maximum values of electrical efficiency attained by small-scale biomass-fired Organic Rankine Cycle (ORC) systems (the leader technology for CHP generation from biomass) are lower than 20%, as reported in [8]. In contrast, CHP plants should be capable of generating more electricity per unit of thermal energy produced, in order to increase the economic feasibility of small-scale plant investments [5]. To reach this target, current research works are primarily focused on both the optimization of ORC parameters (see, e.g., the optimization study proposed in [9]) and the best selection of the available organic fluids (see, e.g., the comparative analysis presented in [10]). Parametric investigations of ORC power plants have also been conducted using novel techno-economic approaches [11].

In this scenario, the aim of this paper is to demonstrate that, thanks to both novel cost-effective configurations proposed here and recent technological advances in designing gas to gas heat exchanger and micro steam expanders, the employment of small combined cycles as a valid alternative to ORC systems for CHP from biomass is feasible in the near future and can guarantee competitive thermodynamic performances. The direct use of solid biomass or low quality biofuels in gas turbines coupled with water steam cycles can be of great interest for a better exploitation of biomass, due to the simplicity, reliability and flexibility of this technical solution. Furthermore, the use of water steam is safe because it has no negative effects on the environment and is not toxic and explosive like some organic molecules; as a result, water steam can also be exhausted and used directly in technological processes or for district heating.

2. Methodology

2.1 Proposal of plant layouts for CHP from biomass

Figure 1 shows the two power plant layouts proposed for CHP from biomass. Both layouts are based on an externally-fired combined cycle: the open Joule Brayton cycle is utilized as the topping, high-temperature plant, and the Rankine cycle as the bottoming, low-temperature plant. The working fluid of the topping cycle is clean air; after being compressed, the air flows through the high temperature heat exchanger, which is necessary to transfer heat from the flue gases exiting the external combustor to the compressed air. In the first plant layout (Fig. 1a), the clean hot air expands in the turbine (T) moving the compressor (C) and the electric generator simultaneously to produce the electrical power of the topping cycle. In the other layout (Fig. 1b), the air expansion is divided into two stages by using two turbines: the high-pressure turbine drives the compressor, while the low-pressure turbine (the power turbine) moves the electric generator.

In both layouts, the hot air discharged from the turbine is conveyed into the external combustor chamber to burn biomass.

The bottoming cycle allows the overall efficiency to be increased. As shown in Fig. 1a and Fig. 1b, the exhaust gases exiting the heat exchanger are delivered to a heat recovery steam generator (HRSG) to generate water steam, which can then expand through a steam expander moving the second electric generator. The steam is expanded to a certain level of back pressure depending on the needs of the thermal load, for instance the temperature of the hot water necessary for district heating. To allow the closed loop, the steam circuit also needs a condenser and a pumping system. Alternatively, the steam can be exhausted from the steam expander and directly used for technological purposes. In such a case, the bottoming plant does not need the condenser and can work in open cycle.

In order to greatly reduce the capital costs, a cheap turbocharger from the automotive industry is proposed to be used in place of the expensive microturbine, considering that automotive turbines are very suitable for this application because nowadays their blades are cast from nickel-alloys to allow high thermal resistance (900-950 °C). Apart from the coupling with the electric generator (which requires a re-design of the shaft and bearings), a turbocharger does not need other modifications to allow its implementation in the plant of Fig. 1a, so this cost-effective technology could successfully be used for serial production of turbocharger-like modules to be connected to electric generators.

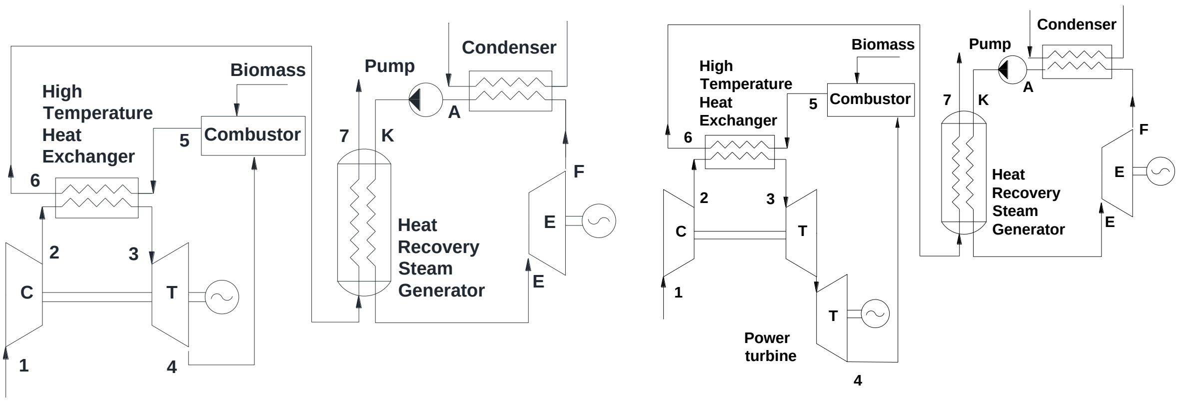

(a) (b)

Figure 1. Plant layouts proposed: turbocharger coupled to the electric generator (a) and turbocharger in series with a downstream power turbine (b)

The direct use of an existing turbocharger, without modifications, is possible in the plant layout of Fig.

1b, in which the shaft of the turbocharger is not coupled to the electric generator. This configuration can give a few advantages during the adjustment of the load, because the high-pressure turbine and the compressor can operate with a wide range of rotational speeds. Despite the use of the additional power turbine, which is commercially available but introduces an additional cost, even this solution is more cost-effective than a standard microturbine.

The biomass combustor can be chosen among available fluidized bed combustors or standard furnaces, which are characterized by good efficiencies (around 90%) thanks to several improvements achieved in the combustion process [12].

With regard to the high temperature heat exchanger, the scientific literature has not highlighted effective gas to gas heat exchangers that are also capable of withstanding very high temperatures [13], therefore the external combustion of solid biomass or low quality bio-fuels has never been performed in combined power plants to date. To overcome this issue, an innovative ceramic exchanger, denominated the Immersed Particle Heat Exchanger (IPHE), has been proposed by the authors and analysed by means of numerical codes and experimental tests [14]. The IPHE is mainly composed of two ceramic columns and employs ceramic particles as intermediate medium to absorb heat from the hot flue gases and to release it to the working fluid (air) exiting the compressor in continuous mode (the particles are collected and delivered back to the top of the plant by using a pneumatic conveyor). The results presented in a previous work [15] showed that this heat exchanger, apart from its capability of withstanding very high temperatures with negligible pressure drops, has the potential to reach an efficiency of 80 % without the necessity of designing bulky columns. Further details about the architecture of the IPHE can be found in [15].

A concrete alternative to the IPHE and ceramic heat exchangers is represented by more traditional heat exchangers made of nickel alloys, which have very high levels of thermal resistance in comparison with other metals; for this reason, nickel alloys are widely used for blades and disks of gas turbines. Among nickel alloys, those based on nickel-chromium seem to be the most effective for this application, because they also guarantee high corrosion resistance [16]. Concerning the cost, it would not be an issue, because the heat exchanger would be very compact, with small size and reduced material content, considering that the flow rates of air and flue gas are very low in this type of power plant. The disadvantage of using a nickel alloy heat exchanger in place of the IPHE is the lower thermal resistance (900-950 ˚C for a nickel alloy) and hence the reduced temperature at the gas turbine inlet, which in turn causes a substantial reduction in the electrical efficiency of the topping cycle.

The steam expander of the bottoming cycle can be selected among recent models of micro-steam turbines, which are more efficient than in the past. For example, the “Green steam turbine” is a commercially available model whose cost amounts to a few thousand Euros and that is capable of generating a maximum electrical power of 15 kW_e , with a maximum pressure of 10 bar and a maximum temperature of 225 °C [17]. Using the data provided by the manufacturer, the isentropic efficiency can be estimated to be equal to about 50%, which represents a high level of performance despite the very low electrical power.

Screw expanders, whose technology is quite mature and has many applications (e.g. ORC cycles and geothermal energy systems), represent an alternative to steam turbines. The peculiar characteristics are the low rotational speed and their ability to operate with large pressure ratios and with wet steam [18]. However, despite manufacturers declare that such motors can operate efficiently even with water steam as working fluid, precise values of the isentropic efficiency are not available in such a case. The effect of a large formation of droplets on the efficiency is not documented as well.

2.2 Optimization process

The performance of the proposed small combined-cycle was investigated by means of an optimization procedure based on a genetic algorithm coupled with a calculation code; particularly, two possible configurations have been considered. The two configurations are equal except for the gas to gas heat exchanger: the first one employs the IPHE, while the other one employs a NAHE. For both cases, the plant layout is the same as Fig.1a, with steam being expanded to 1 bar in order to allow high temperature heat recovery from its condensation (100 °C). Furthermore, the turbocharger Garrett GTX5518R [19] was selected because it is appropriate to achieving an electrical power of about 100 kW, given the values of flow rate, pressure ratio and maximum temperature allowed by the turbine material (nickel alloy).

The "Green steam turbine" [17], by virtue of its high efficiency and low cost, was chosen as the steam expander of the bottoming cycle. The steam must be superheated to avoid pitting and corrosion, thus preserving the integrity of the turbine.

Five design parameters, namely the parameters whose values have to be optimized, were selected: the mass flow rate of air, G_a, the pressure ratio of the compressor, β, the temperature and pressure of steam at the inlet of the steam turbine, T_E and p_E (see Fig. 1 for the meaning of the subscripts), and the efficiency of the heat exchanger, ε.

These parameters were allowed to vary within quite a large design space, as reported in Table 1.

DESIGN PARAMETER	***LOWER BOUND***	***UPPER BOUND***	***STEP***
Mass flow rate of air, G_a (kg/sec)	*0.3780 (50 lb/min)*	*1.134 (150 lb/min)*	*0.03780 (5 lb/min)*
Pressure ratio (turbocharger), β	*2.2*	*3.5*	*0.1*
Steam expander inlet temperature, T_E (°C)	*150*	*225*	*5*
Steam expander inlet pressure, p_E (bar)	*5*	*10*	*0.1*
Efficiency of the heat exchanger, ε	*0.5*	*0.8*	*0.01*

Table 1 – Design parameters for both configurations

The upper bounds of T_E and p_E result from the limits of temperature and pressure of the "Green steam turbine". The lower and upper bounds of G_a and β are consistent with the maps of the turbocharger. The maximum efficiency of the heat exchanger was assumed equal to 0.8, in order to avoid an extreme design of this component for higher values of the efficiency [15].

With regard to the choice of the objective functions, the electrical efficiency, η_{el} , and the thermal efficiency, η_{th} , were selected as the objectives to be maximized by the optimization algorithm. The choice of maximizing η_{th} and η_{el} rather than maximizing only one parameter, e.g. the overall efficiency ($\eta_{tot} = \eta_{th} + \eta_{el}$) or the Primary Energy Savings (PES), was made because this bi-objective strategy allows for analysing the trade-off between the maximization of the electrical efficiency and the maximization of the thermal efficiency, so as to explore the potential of the proposed configurations in detail.

The search for the best combination of the design parameters cannot be carried out regardless of its technological feasibility; for this reason, an individual was considered unfeasible and consequently discarded by the optimization algorithm if the following constraints were not satisfied:

1) the dryness fraction of steam, x_s, at the exit of the steam turbine must be higher than 95% to avoid the formation of a large quantity of droplets inside the expander;

2) the temperature of the exhaust gas exiting the HRSG, T_7, must be higher than 150 °C to avoid the formation of acid rain caused by the sulphur content of biomass, typically 0.1 - 1%;

3I) the temperature of the air at the gas turbine inlet, T_3, must be lower than 900 °C in the configuration with the IPHE to preserve the integrity of the turbine (configuration I);

3II) the temperature of the flue gases at the exit of the external combustor, T_5, must be lower than 900°C in the configuration with the NAHE to preserve the integrity of the heat exchanger (configuration II).

A summary of the constraints and objectives employed for the two optimization designs is reported in Table 2 for completeness.

Optimization	***Objectives***	***Constraint 1***	***Constraint 2***	***Constraint 3***
Configuration I (IPHE)	*Maximize* η_{th} and η_{el}	$x_s > 95\%$	$T_7 > 150$ °C	$T_3 < 900$ °C
Configuration II (NAHE)	*Maximize* η_{th} and η_{el}	$x_s > 95\%$	$T_7 > 150$ °C	$T_5 < 900$ °C

Table 2 – Objectives and constraints

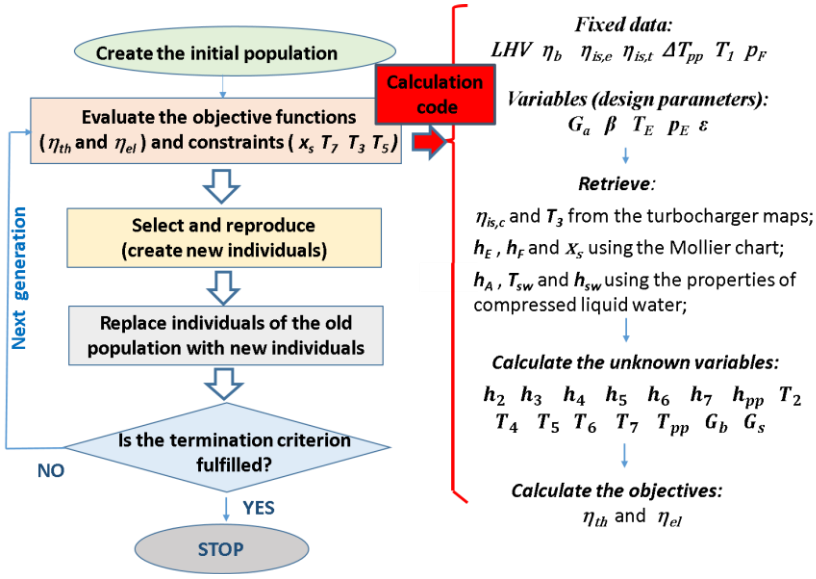

Figure 2. Flow chart of the optimization process, where the symbols refer to Fig. 1a

The optimization process consisted of a sequential process implemented in the modeFRONTIER software, in which a calculation code was coupled with an effective genetic algorithm, MOGAII [20]. Unlike gradient based methods (see, e.g., an efficient gradient based optimization proposed in [21]), a genetic algorithm is based on the evaluation of a set of individuals (population), which is varied at each iteration making use of operations of selection, cross-over, and random mutation to determine the set of the best individuals [20]. MOGA II has general validity and was successfully tested by the authors of this paper in [22] for the fluid dynamic design optimization of hydraulic proportional valves [23]. Further details regarding MOGAII and the optimization parameters (not reported here for brevity) can be found in [22]. The flow chart of the optimization process is reported in Figure 2. The process was stopped after 10000 individuals had been explored (termination criterion).

2.3 Thermodynamic modelling

A calculation code was implemented in the optimization process to calculate the objective functions (η_{th} and η_{el}) and the constraints (x_s , T_7 , T_3 , T_5) for each combination of the design parameters (see Fig. 2). Starting from the known values of the design parameters (G_a, β, T_E, p_E , ε), the code can calculate the enthalpy and temperature at each section of the plant (see Fig. 1a) as well as the mass flow rates of fuel (G_b) and steam (G_s) in order to evaluate the objectives and constraints. The calculation was performed by assuming that the specific heat capacity at constant pressure (c_p) was a cubic function of temperature [24] (the four coefficients of the flue gases were assumed equal to the air coefficients); the maps of the turbocharger, the Mollier chart and the thermodynamic properties of water were implemented in the code, which also made use of the energy balances in the combustor, in the heat exchanger and in the HRSG. Denoting the efficiency of the combustion by η_b, the energy balance in the combustor is given by:

$$\eta_b\, G_b\, LHV + G_a\, h_4 + G_b\, h_b \;=\; (G_a + G_b) h_5 \tag{1}$$

where h_b is the initial enthalpy of the fuel, h_4 is the enthalpy of the air at the inlet of the combustor and h_5 is the enthalpy of the flue gases at the outlet of the combustor. With regard to the energy conservation in the heat exchanger (assumed adiabatic), the following equation holds:

$$G_a\,(h_3 - h_2) = (G_a + G_b)(h_5 - h_6) \tag{2}$$

with h_2 , h_3 being the air enthalpies at the inlet and outlet of the heat exchanger, respectively, and h_6 being the enthalpy of the flue gases at the exit of the heat exchanger. The efficiency of the heat exchanger is in relation with the enthalpies through the following expression:

$$\varepsilon \,= \frac{(h_3 - h_2)}{(h_5 - h_2)} \tag{3}$$

Finally, the heat exchange between the flue gases and the water-steam in the HRSG can be expressed by equations 4 and 5:

$$G_s(h_E - h_{sw}) = (G_a + G_b)\big(h_6 - h_{pp}\big) \tag{4}$$

$$G_s(h_E - h_k) = (G_a + G_b)(h_6 - h_7) \tag{5}$$

where h_E, h_{sw} and h_k are the enthalpies of the superheated steam, saturated water and compressed water entering the HRSG, respectively; h_7 denotes the enthalpy of the flue gases exiting the HRSG; h_{pp} is the enthalpy of the flue gases at the pinch point, where the temperature of the flue gases (T_{pp}) is given by:

$$T_{pp} = T_{sw} + \,\Delta\, T_{pp} \tag{6}$$

with T_{sw} and ΔT_{pp} denoting the temperature of the saturated water and the pinch point temperature difference, respectively.

The objectives (η_{el} and η_{th}) were calculated as follows:

$$\eta_{el} = \frac{P_{el}}{\mathrm{G_b} LHV} = \frac{P_{el,top} + P_{el,bot}}{\mathrm{G_b} LHV} = \frac{G_a[\eta_{m,t}(h_3 - h_4) - \frac{(h_2 - h_1)}{\eta_{m,c}}] + \eta_{m,e} G_s(h_E - h_F)}{\mathrm{G_b} LHV} \tag{7}$$

$$\eta_{th} = \frac{P_{th}}{G_b LHV} = \frac{G_S(h_F - h_A)}{G_b LHV} \quad (8)$$

where P_{el}, $P_{el,top}$, $P_{el,bot}$ and P_{th} are the overall electrical power, the electrical power of the topping cycle, the electrical power of the bottoming cycle and the useful thermal power, respectively; h is the specific enthalpy and subscripts *1, 2, 3, 4, E, F, A* denote the corresponding sections of the plant shown in Fig.1a; $\eta_{m,c}$, $\eta_{m,t}$ and $\eta_{m,e}$ are the mechanical efficiencies of the compressor, turbine and expander, respectively. The assumptions reported in Table 3 were used for the calculations, specifically: the *LHV* of biomass, the back pressure of the steam turbine (p_F) and the pinch point temperature difference (ΔT_{pp}) were set equal to 19000 kJ/kg, 1 bar, and 15 K, respectively. In addition, the combustor efficiency (η_b) was assumed equal to 0.9 (according to the current technology) and the mechanical efficiencies of the compressor and the turbines ($\eta_{m,c}$, $\eta_{m,t}$ and $\eta_{m,e}$) were set equal to 0.98. The isentropic efficiencies of the expander ($\eta_{is,e}$) and the turbine of the turbocharger ($\eta_{is,t}$) were considered constant and equal to 0.5 (see Section 2.1) and 0.82 (data retrieved from the map of the turbine), respectively, because their variations in the design space are negligible. The ambient temperature (T_1) was supposed to be equal to 15ºC and the pressure drop through the heat exchanger was considered negligible.

Setting	VALUE
c_p	$c_p(T) = a + b\,T + c\,T^2 + d$
LHV	*19000 kJ/kg*
p_F	*1 bar*
ΔT_{pp}	*15 K*
η_b	*0.9*
$\eta_{is,e}$	*0.5*
$\eta_{is,t}$	*0.82*
$\eta_{m,t} = \eta_{m,c} = \eta_{m,e}$	*0.98*
T_1	*15 °C*

Table 3 – Assumptions for the calculations

3. Results

3.1 Results of the optimization process

The charts of Figure 3 and Figure 4 display all the feasible individuals (combinations of the design parameters that respect the prescribed constraints) within the objective function space of Configuration

I (IPHE) and Configuration II (NAHE), respectively. Each feasible individual is plotted as a point at the location specified by its values of η_{th} and η_{el} : the points are also coloured accordingly to the value of the overall efficiency (blue represents lower values, red upper values). It is noteworthy that the feasible points are uniformly distributed in the objective space, thus demonstrating the flexibility of both configurations.

Among the feasible individuals, it is possible to observe the set of those individuals that are not dominated by any others, namely the "*Pareto-front*", which represents the limit beyond which the design cannot further be improved. In Figures 3 and 4 some points are black marked: these points represent the individuals that satisfy all the constraints but for which the electric power of the bottoming cycle is greater than the maximum power of the "Green steam turbine" (15 kW). For these individuals, a micro-steam turbine similar to the "Green steam turbine" but capable of generating more electrical power, specifically up to 22 kW (the maximum steam power registered), must be selected among commercially available turbines.

As expected, it is not possible to choose an individual belonging to the front that is capable of maximizing η_{th} and η_{el} at the same time, because the maximization of η_{el} causes the reduction in η_{th} , and vice versa; as a result, the optimum must be chosen according to which form of energy must be favoured and to what extent. If the final objective is the maximization of the overall efficiency, the optimum individual must be the element of the Pareto front for which the sum of η_{th} and η_{el} is the maximum possible.

As shown in the charts of Figures 3 and 4, the configuration with the NAHE has the potential to reach a maximum electrical efficiency of about 0.22, while the configuration with the IPHE can attain a maximum electrical efficiency of about 0.25: this improvement is due to the higher temperature at the gas turbine inlet occurring when the IPHE is used. In both cases, the electrical efficiency is higher than that of a typical biomass-fuelled ORC system, whose electrical efficiency is usually well below 0.2. This is a very important achievement, because, as discussed earlier, it is important to design new CHP power plants characterized by high values of electrical efficiency in order to increase the amount of electrical energy produced per total biomass energy input, thus allowing a better exploitation of biomass.

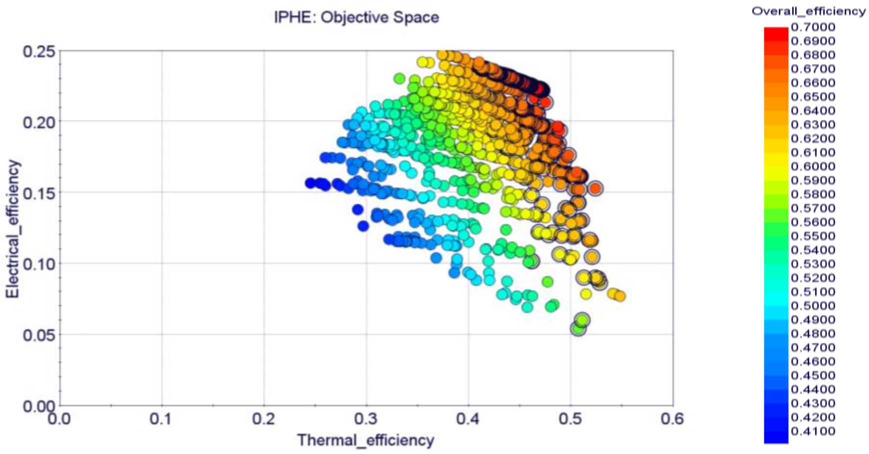

Figure 3. Objective space (feasible individuals), Configuration I (IPHE)

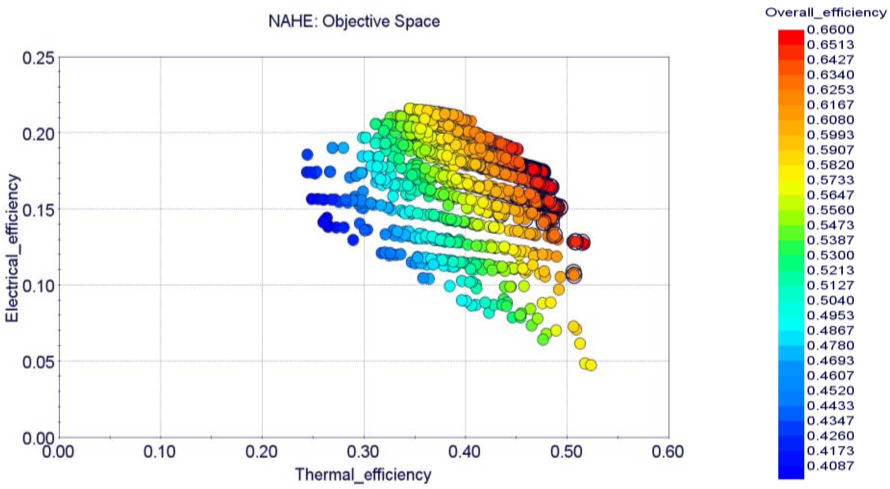

Figure 4. Objective space (feasible individuals), Configuration II (NAHE)

To provide a detailed analysis of the potential of the combined cycle proposed, Figures 5 and 6 report all the feasible individuals in the Electrical power (P_{el}) –Thermal power (P_{th}) Space of Configuration I (IPHE) and Configuration II (NAHE), respectively. The electrical efficiency is also indicated for each individual by means of a colour scale. From the comparison of Figure 5 and Figure 6, it results that, as expected, Configuration I has the potential to reach higher values of both P_{el} and P_{th} compared to Configuration II (this is due to the higher enthalpy at the gas turbine inlet allowed by the IPHE). In both cases, a large combination of P_{el} and P_{th} with high η_{el} (e.g. higher than 20%) is possible, thus demonstrating the flexibility of both solutions once again.

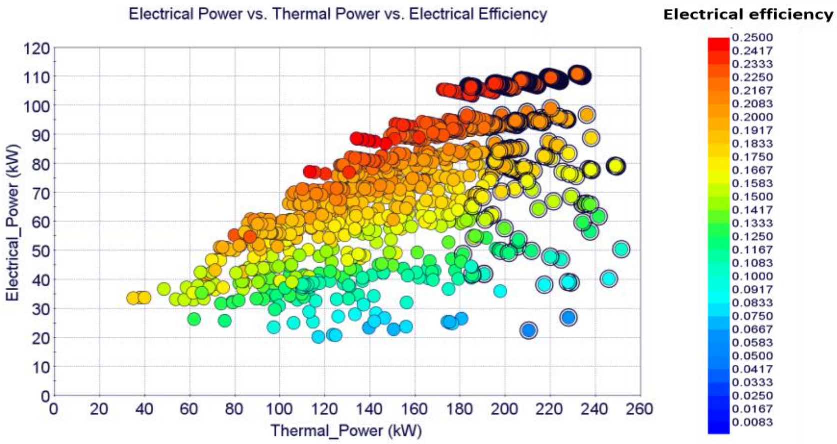

Figure 5. Electrical Power vs Thermal power vs Electrical Efficiency (feasible individuals), Configuration I (IPHE)

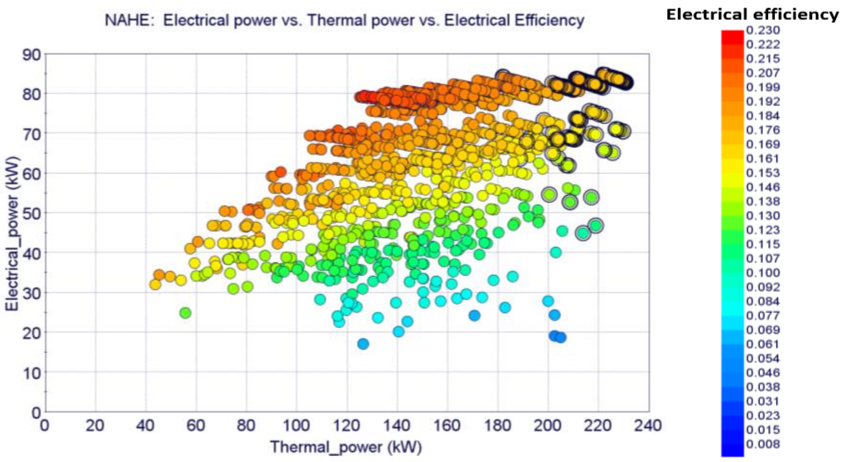

Figure 6. Electrical Power vs Thermal power vs Electrical Efficiency (feasible individuals), Configuration II (NAHE)

Table 4 reports the design parameters, thermal parameters and efficiencies of the individuals characterized by the highest values of η_{el} , η_{tot} and η_{th} for both configurations. The examination of the design parameters of the two individuals characterized by the highest values of η_{el} (0.2471 for Configuration I and 0.2160 for Configuration II) reveals that, in order to achieve this target, the optimizer found two combinations of G_A and β for which T_3 and T_5 are very close to the maximum possible values (see constraints 3 in Table 2); in addition, the efficiency of the heat exchanger was increased to the upper bound (0.8) in order to maximize the efficiency of the topping cycle. The values of the pressure and temperature of the superheated steam were set equal to the upper bounds (10 bar and 225 °C), so as to optimize the efficiency of the bottoming cycle as well.

With regard to the individual having the maximum thermal efficiency, its value is 0.5479 for Configuration I (IPHE) and 0.5233 for Configuration II (NAHE). However, the electrical efficiency is too low in this case (0.07713 for Configuration I and 0.04764 for Configuration II), so these combinations of the design parameters are not a good choice. Nevertheless, this case has been presented to better recognize the influence of the design parameters upon the objectives. It is noteworthy that, in order to achieve the maximum thermal efficiency, the optimizer chose a combination of G_A and β for which T_3 is very low, while the efficiency of the heat exchanger was lowered to the minimum possible value (0.5) so as to penalize the efficiency of the topping cycle, thus increasing the heat recovery in the bottoming cycle. The comparison with the former case leads to the conclusion that the efficiency of the heat exchanger plays an important role in the trade off between the electrical power and the thermal power, and the highest heat exchange efficiency will be mandatory only if the objective is the maximization of the electrical power.

With regard to the two individuals characterized by the highest values of η_{tot} (0.6933 for Configuration I and 0.6543 for Configuration II), Table 4 shows that the efficiency of the heat exchanger was slightly reduced in comparison with the two individuals characterized by the highest values of η_{el}, so as to increase T_6 and hence the thermal power transferred to the steam in the HRSG. In this case, the combinations of p_E and T_E result from the limits imposed both to the dryness fraction of steam (see constraint 1 in Table 2) and to the temperature of the exhaust gases exiting the HRSG, T_7 (see constraint 2 in Table 2); in particular, T_7 was decreased to the minimum allowed value (423 K) so as to increase the production of water steam. In this case, the electric power of the bottoming cycle is greater than 15 kW (the maximum power of the “Green steam turbine”), so another steam turbine must be either selected among those available or properly designed. It is noteworthy that, in the configuration with the NAHE, the optimizer has favoured the thermal efficiency (equal to 0.4815*)* rather than the electrical efficiency (equal to 0.1728). However, as shown in Figures 4 and 6, there are other possible combinations of η_{el} and η_{th} that can lead to η_{tot} > 0.60 with η_{el} > 0.2.

		Maximum η_{el}		*Maximum η_{tot}*		*Maximum η_{th}*	
		Conf. I (IPHE)	Conf. II (NAHE)	Conf. I (IPHE)	Conf. II (NAHE)	Conf. I (IPHE)	Conf. II (NAHE)
Design Parameters							
G_a	*kg/s*	*0.6804*	*0.7940*	*0.7940*	*0.8694*	*0.6426*	*0.9072*
β	-	*3*	*3.3*	*3.5*	*3.5*	*2.2*	*3*
ε	-	*0.8*	*0.8*	*0.75*	*0.7*	*0.5*	*0.5*
p_E	*bar*	*10*	*10*	*9*	*7.5*	*8.75*	*6.5*
T_E	*°C*	*225*	*225*	*215*	*205*	*195*	*210*
Constraints							
T_3	*K*	*1152*	*1024.1*	*1152*	*960.4*	*694.6*	*648.0*
T_5	*K*	*1320*	*1160.6*	*1369*	*1165*	*990.0*	*863.1*
T_7	*K*	*439.3*	*444.6*	*423*	*423.1*	*424.4*	*424.6*
x_s	-	*1*	*1*	*0.9978*	*0.999*	*0.9813*	*1*
Thermal parameters							
$\eta_{is,c}$	-	*0.75*	*0.76*	*0.75*	*0.765*	*0.79*	*0.79*
G_s	*kg/s*	*0.0593*	*0.0563*	*0.104*	*0.102*	*0.0796*	*0.08980*
G_b	*kg/s*	*0.0189*	*0.01936*	*0.0261*	*0.0252*	*0.0169*	*0.0206*
T_2	*K*	*429.6*	*442.05*	*453.1*	*449.9*	*370.8*	*422.5*
T_4	*K*	*923.5*	*802.2*	*900.5*	*738.2*	*588.8*	*509.3*
T_6	*K*	*640.6*	*608.7*	*720*	*689.9*	*702.3*	*652.8*
$G_b \cdot LHV$	*kW*	*358.5*	*367.9*	*496.5*	*479.2*	*191.4*	*391.3*
$P_{el,top}$	*kW*	*76.54*	*68.1*	*89.78*	*64.81*	*10.10*	*3.773*
$P_{el,bot}$	*kW*	*12.05*	*11.36*	*20.03*	*17.98*	*14.73*	*14.87*
P_{el}	*kW*	*88.6*	*79.45*	*109.8*	*82.79*	*24.83*	*18.64*
P_{th}	*kW*	*134*	*127*	*234*	*231*	*176.4*	*204.8*
P_{th} / P_{el}	-	*1.513*	*1.5941*	*2.1344*	*2.787*	*7.103*	*10.98*
Performance							
$\eta_{el,top}$	-	*0.2134*	*0.185*	*0.1808*	*0.1352*	*0.03138*	*0.009640*
$\eta_{el,bot}$	-	*0.08238*	*0.08219*	*0.0786*	*0.0722*	*0.07694*	*0.06761*
η_{el}	-	***0.2471***	***0.2160***	*0.2212*	*0.1728*	*0.07713*	*0.04764*
η_{th}	-	*0.3738*	*0.3443*	*0.4611*	*0.4815*	***0.5479***	***0.5233***
η_{tot}	-	*0.6210*	*0.5603*	***0.6933***	***0.6543***	*0.6250*	*0.5710*
PES	-	*0.3130*	*0.227*	*0.3156*	*0.2266*	*-0.0665*	*-0.1839*

Table 4 – Parameters and efficiencies for the maximum η_{el} , η_{tot} and η_{th}

An important index of performance is the Primary Energy Saving (PES), which estimates the total energy saving that is possible to achieve by a cogeneration unit when compared with the separate generation of heat and power [25]. The PES values are reported in Table 4 and were calculated, assuming the reference electrical efficiency (denoted by $\eta_{el,ref}$) equal to 0.25 and the reference thermal efficiency ($\eta_{th,ref}$) equal to 0.8 (according to the guidelines of The European Directive 2004/8/EC [25]), as follows:

$$PES = 1 - \frac{1}{\frac{\eta_{el}}{\eta_{el,ref}} + \frac{\eta_{th}}{\eta_{th,ref}}} \tag{9}$$

The European Directive 2004/8/EC states that a new CHP plant can be classified as a high efficiency system if the primary energy saving is greater than 10% [25]. As shown in Table 4, the potential of the proposed plant is well above this limit, with the primary energy saving being equal to about 31% in Configuration I and 22% in Configuration II.

3.2 Results of the load following assessment

This section deals with the assessment of the load following capability of the proposed combined cycle. The compressor is not equipped with variable guide vanes, therefore the power level must be adjusted by only acting on the fuel flow. Several control algorithms capable of adjusting the fuel flow rate with high precision are available [26].

As discussed in Section 3.1, if the goal is to convert biomass into electricity more efficiently than other small CHP power plants, the operating parameters of the proposed power plant must be set equal to the design parameters of the individual characterized by the maximum value of η_{el} (see Table 4). In such a case, the performance of the power plant at partial load is shown in Figures 7 and 8, which report the operational field in the P_{th} - P_{el} space and the electrical efficiency at partial load, for Configuration I (IPHE) and Configuration II (NAHE) respectively.

The points at partial load were obtained by utilizing the thermodynamic model described in Section 2.3 with the assumption that the turbine must rotate at constant speed (note that a gear reducer needs to be interposed between the turbine and the electric generator because of the lower speed of the latter). The operating point (G_a , β) was moved along the constant speed curve (RPM = 71000 for Configuration I and RPM = 75000 for Configuration II) in the compressor map, while maintaining P_E=10 bar , T_E = *225°C* and ε = 0.8. In both cases, the electrical output was changed from the full load to 25% of the full load and the results can apply both to thermal load and to electric load following. The operating line in the P_{th} - P_{el} space represents the maximum thermal power achievable for a fixed value of electrical power, while the zone under this line represents the operating conditions for which the excess thermal power can be dissipated by opening a by-pass system. It can be noted that, as occurs in ORC systems, the reduction in load causes a consequential reduction in the electrical efficiency, and this is the reason why a biomass-fuelled CHP plant is best suited for operating at its base load. However, it is noteworthy that configuration I (IPHE) can guarantee a high electrical efficiency even at 50% of the full load, thus allowing the effective utilization of the proposed power plant not only for base-load electrical demand but also for variable thermal and/or electric load demand. The configuration with the NAHE can also be used as load following power plant effectively; however, in such case, power changes must be limited to 2/3 of the full load to avoid a high decrease in the electrical efficiency.

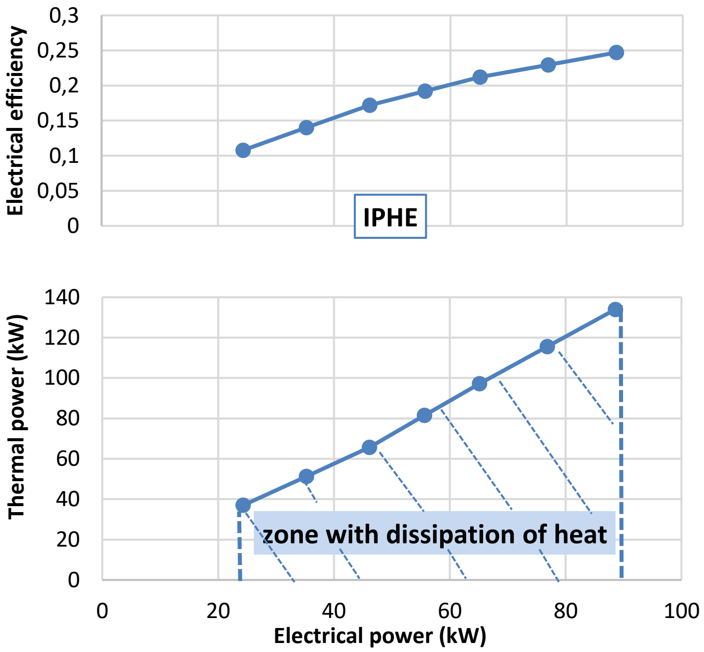

Figure 7. Thermal power (bottom) and Electrical efficiency (top) vs Electrical power for the individual with the maximum efficiency of Configuration I (IPHE)

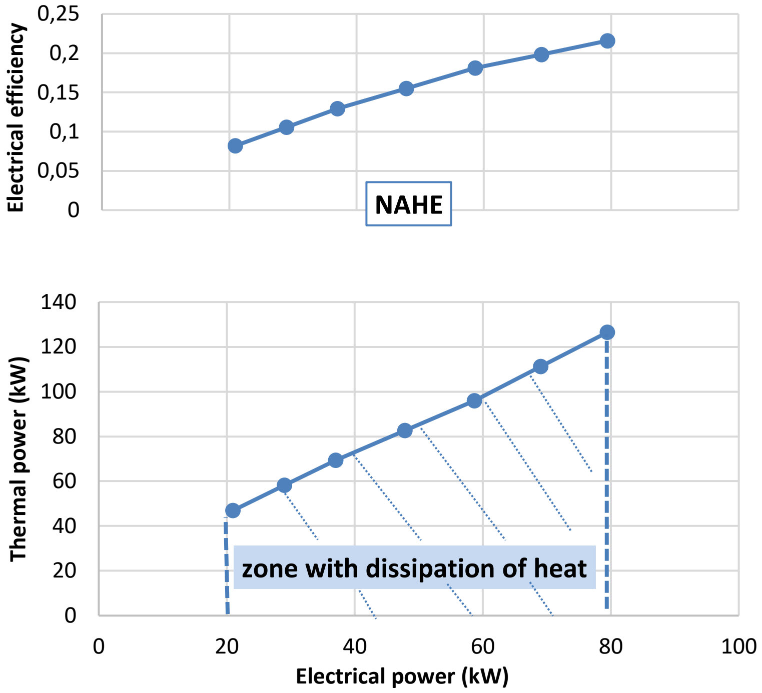

Figure 8. Thermal power (bottom) and Electrical efficiency (top) vs Electrical power for the individual with the maximum efficiency of Configuration II (NAHE)

4. Conclusions

The aim of this paper was to demonstrate the feasibility of small combined cycles for CHP generation from biomass by proposing novel configurations that are cost-effective and perform well. In the configurations proposed, the expensive microturbine is replaced by a cheap automotive turbocharger, which can be either directly connected to the electric generator or coupled with a commercial power turbine suited for generating the electrical power. Solid biomass or low quality biofuels are burned in an external combustor, and the heat exchange between the dirty flue gas and the working fluid of the topping cycle (air) can be performed by either the IPHE or a NAHE. In the bottoming cycle, the HRSG captures the residual heat from the high temperature exhaust gases to produce water steam; the steam expander can be selected among recent models of micro-steam turbines or volumetric expanders, which are more reliable and effective than in the past.

An optimization procedure, based on a genetic algorithm coupled with a calculation code, was utilized to study the performance of a combined cycle employing a turbocharger-like module and the "Green steam turbine", capable of generating up to 15 kW with an isentropic efficiency of 50%. To avoid pitting and corrosion with significant damages to the blades of the turbine, the HRSG must be equipped with a superheater. Two design optimizations were performed according to two different configurations, which are equal expect for the gas to gas heat exchanger employed, namely the IPHE or the NAHE. In both configurations, the steam is expanded to 1 bar in order to allow high temperature heat recovery from its condensation (100 °C). In order to explore the potential of the proposed configurations, the thermal efficiency and the electrical efficiency were selected as the objectives to be maximized by the optimization algorithm. The results of the optimization process have shown that the configurations with the IPHE and with the NAHE have the potential to reach a maximum electrical efficiency of about 0.25 and 0.22, respectively. Concerning the maximum overall efficiency, a considerable value of 0.7 can be achieved with the IPHE and 0.65 with the NAHE. The performance in terms of primary energy saving (PES) is also very high in both cases, with the PES value being above 30% with the IPHE. Finally, it was demonstrated that both configurations can effectively be used not only in base load applications, but also in load following mode; in particular, it was shown that the configuration with the IPHE can guarantee a high efficiency (about 20%) even at 50% of the full load.

A pilot plant for both configurations will be built, by means of a project funded by Apulia Region, at the LabZero Research Centre of Polytechnic University of Bari in the south of Italy. The design of the IPHE and the NAHE will be provided in part II of this paper.

Acknowledgements

This work has been supported by "Regione Puglia" under contract LabZero Research.

References

1. Demirbas, M. F., Balat, M., & Balat, H. (2009). Potential contribution of biomass to the sustainable energy development. Energy Conversion and Management, 50(7), 1746-1760.
2. Amelio, M., Morrone, P., Gallucci, F., & Basile, A. (2007). Integrated gasification gas combined cycle plant with membrane reactors: technological and economical analysis. Energy Conversion and Management, 48(10), 2680-2693.
3. Loha, C., Chatterjee, P. K., & Chattopadhyay, H. (2011). Performance of fluidized bed steam gasification of biomass–modeling and experiment. Energy Conversion and Management, 52(3), 1583-1588.
4. García Fernández, R., Pizarro García, C., Gutiérrez Lavín, A., Bueno de las Heras, J. L., & Pis, J. J. (2013). Influence of physical properties of solid biomass fuels on the design and cost of storage installations. Waste management, 33(5), 1151-1157.
5. Dong, L., Liu, H., & Riffat, S. (2009). Development of small-scale and micro-scale biomass-fuelled CHP systems–A literature review. Applied thermal engineering, 29(11), 2119-2126.
6. Borsukiewicz-Gozdur, A., Wiśniewski, S., Mocarski, S., & Bańkowski, M. (2014). ORC power plant for electricity production from forest and agriculture biomass. Energy Conversion and Management, 87, 1180-1185.
7. Wright, D. G., Dey, P. K., & Brammer, J. (2014). A barrier and techno-economic analysis of small-scale bCHP (biomass combined heat and power) schemes in the UK. Energy, 71, 332–345.
8. Capata, R., & Toro, C. (2014). Feasibility analysis of a small-scale ORC energy recovery system for vehicular application. Energy Conversion and Management, 86, 1078-1090.
9. Wei, D., Lu, X., Lu, Z., & Gu, J. (2007). Performance analysis and optimization of organic Rankine cycle (ORC) for waste heat recovery. Energy conversion and Management, 48(4), 1113-1119.

10. Dai, Y., Wang, J., & Gao, L. (2009). Parametric optimization and comparative study of organic Rankine cycle (ORC) for low grade waste heat recovery. Energy Conversion and Management, 50(3), 576-582.
11. Zhang, C., Shu, G., Tian, H., Wei, H., & Liang, X. (2015). Comparative study of alternative ORC-based combined power systems to exploit high temperature waste heat. Energy Conversion and Management, 89, 541-554.
12. Dare, P., Gifford, J., Hooper, R. J., Clemens, A. H., Damiano, L. F., Gong, D., & Matheson, T. W. (2001). Combustion performance of biomass residue and purpose grown species. Biomass and Bioenergy, 21(4), 277-287.
13. Jeong, J. H., Kim, L. S., Lee, J. K., Ha, M. Y., Kim, K. S., & Ahn, Y. C. (2007, January). Review of heat exchanger studies for high-efficiency gas turbines. In ASME Turbo Expo 2007: Power for Land, Sea, and Air (pp. 833-840). American Society of Mechanical Engineers.
14. Catalano, L. A., De Bellis, F., Amirante, R., & Rignanese, M. (2011). An immersed particle heat exchanger for externally fired and heat recovery gas turbines. Journal of Engineering for Gas Turbines and Power, 133(3), 032301.
15. Amirante, R., & Tamburrano, P. (2014). High Temperature Gas-to-Gas Heat Exchanger Based on a Solid Intermediate Medium. Advances in Mechanical Engineering, 2014.
16. Stein-Brzozowska, G., Flórez, D. M., Maier, J., & Scheffknecht, G. (2013). Nickel-base superalloys for ultra-supercritical coal-fired power plants: Fireside corrosion. Laboratory studies and power plant exposures. Fuel, 108, 521-533.
17. Green Turbine™ http://www.greenturbine.eu/GT15.html. 2009 (accessed 3/9/2014).
18. Smith, I. K., Stosic, N., & Kovacevic, A. (2005). Screw expanders increase output and decrease the cost of geothermal binary power plant systems. Transactions of Geothermal Resource Council, Reno, NV, September, 25-28.

19. Honeywell International http://www.turbobygarrett.com/turbobygarrett/turbochargers. 2012 (accessed 3/9/2014).
20. Poloni, C., & Pediroda V. (1997). GA Coupled with Computationally Expensive Simulations: Tools to Improve Efficiency. In Genetic Algorithms and Evolution Strategies in Engineering and Computer Science, 267-288. New York: JohnWiley & Sons.
21. Amirante, R., Catalano, L. A., Dadone, A., & Daloiso, V. S. E. (2007). Design optimization of the intake of a small-scale turbojet engine. CMES - Computer Modeling in Engineering and Sciences, 18(1), 17-30.
22. R. Amirante, L.A. Catalano, C. Poloni, & P. Tamburrano. (2014). Fluid-dynamic design optimization of hydraulic proportional directional valves. Engineering Optimization, 46 (10), 1295-1314.
23. Amirante, R., Distaso, E., & Tamburrano, P. (2014). Experimental and numerical analysis of cavitation in hydraulic proportional directional valves. Energy Conversion and Management, 87, 208-219.
24. Cengel, Y. A. (2007). Introduction to Thermodynamics and Heat Transfer (pp. 253-262). New York: McGraw Hill Higher Education Press.
25. Ferreira, A., Nunes, M.L., Teixeira, S., & Martins, L.B. (2014).Technical-economic evaluation of a cogeneration technology considering carbon emission savings. International Journal of Sustainable Energy Planning and Management, 2, 33-46.
26. Amirante, R., Catalano, L. A., & Tamburrano, P. (2012). Thrust control of small turbojet engines using fuzzy logic: Design and experimental validation. Journal of Engineering for Gas Turbines and Power, 134 (12).